Archives of Materials Science and Engineering

Volume 28
Issue 11
November 2007
Pages 677-682

International Scientific Journal
published monthly as the organ of
the Committee of Materials Science
of the Polish Academy of Sciences

Compaction of the diamond – Ti_3SiC_2 graded material by the high – speed centrifugal compaction process

V. Mityushev [a], L. Jaworska [b,c,*], M. Rozmus [c], B. Królicka [b]

[a] Department of Mathematics, Pedagogical Academy,
ul. Podchorążych 2, 30-084 Kraków, Poland
[b] Department of Techniques, Pedagogical Academy,
ul. Podchorążych 2, 30-084 Kraków, Poland
[c] Institute of Advanced Manufacturing Technology,
ul. Wrocławska 37A, 30-011 Kraków, Poland
* Corresponding author: E-mail address: lucyna.jaworska@ios.krakow.pl

Received 15.10.2007; published in revised form 01.11.2007

ABSTRACT

Purpose: Sedimentation of particles in a viscous fluid is a main physical problem in fluid mechanics. Sedimentation is benchmark of one of the technica; methods to produce the functionally graded materials (FGM) with a continuous spatial change of mechanical properties. The aim of the research was execution of mathematical calculations of the phases distribution for the phase graded diamond-Ti_3SiC_2 compacts which were verified with phases distribution in compacts after the high pressure – high temperature sintering process.

Design/methodology/approach: In this paper, we construct a mathematical model of FGM basing on the modifications of the Stokes formula. We proposed an algorithm to describe sedimentation of the group of spherical particles of different sizes and different materials. Main calculations for this system and real conditions of the high-speed centrifugal compaction process are made using the Barnea-Mizrahi equation. Deposition process was carried out using the ultra centrifuge UP 65M with rotational speed of 15000 to 25000 rpm. Particle size distribution for the diamond and Ti_3SiC_2 powders were measured using Shimadzu apparatus.

Findings: The results of calculations and microscopic analysis are compared. The obtained results of mathematical calculations demonstrate that for the considered diamond-Ti_3SiC_2 suspensions the obtained compact has the structure of the laminate what confirmed microscopic analysis.

Practical implications: The mathematical simulations using our algorithm show that it is possible to obtain continuous concentrations of the both materials with appropriate initial suspensions. Thus our method allows to obtain graded materials.

Originality/value: This mathematical model gives possibility of use to describe sedimentation of the group of spherical particles different materials and different sizes.

Keywords: High-speed centrifugal compaction process; Sedimentation; Barnea-Mizrahi equation

MATERIALS MANUFACTURING AND PROCESSING

1. Introduction

Sedimentation of particles in a viscous fluid is a classical physical problem in fluid mechanics. It is the benchmark of one of the technical methods to produce laminates, in particular, the functionally graded materials (FGM) with a continuous spatial change of mechanical properties [1,2,3,4,5]. Such materials have advantages on the classic laminates and other composites, because the interface between phases yields jumps in the thermal expansion and the elastic modulus of media. In the same time, FGM create a slowly changing gradient of the thermoelastic properties in media. Hence, the thermal flux and the stress tensor change also slowly in such materials.

A single heavy spherical particle falls in a viscous fluid under the gravitational field according to the Stokes settling velocity [6]

$$U_s = \frac{d^2(\rho - \rho_c)}{18\eta} g_0, \tag{1}$$

where d denotes the diameter of the sphere, ρ and ρ_c the densities of the particles and of the fluid, η the dynamic viscosity of the fluid, g_0 the gravitational acceleration. Formula (1) is valid for laminar flow when the Reynolds number $\mathrm{Re} = \frac{U_s \rho d}{\eta}$ satisfies the inequality $10^{-4} < \mathrm{Re} < 2$ [6]. The latter restriction holds for slowly falling particles.

We now briefly present recent theoretical and experimental works devote to different aspects of sedimentation. R. B. Jones & R. Kutteh [7] applied the Stokesian simulations to compare the hydrodynamic interactions between colloidal particles in unbounded fluid and near a hard wall. The results showed that particles in unbounded fluid there is a high degree of symmetry in the configuration of the particles which is broken by the presence of the walls. A similar method based on statistical mechanics were used in [8] to study random clouds of the particles. The gravitational settling of small particles were numerically investigated in [9]. The effect of side walls on the velocity fluctuation were investigated theoretically in [10,11] and experimentally in [12,13]. A model of the velocity fluctuation were presented in [14]. This model showed that there is a critical stratification above which velocity fluctuations changed significantly. Lattice-Boltzmann simulation were applied to monodisperse and polydisperse suspensions [15]. It was verified that particle velocity fluctuations were suppressed by no-slip condition on the walls. Kynch's cinematic sedimentation model applied to high concentration suspensions and its generalizations are described in [16]. One can also find a review of recent experimental and theoretical works in [17]. It follows from the above review that the significant success has been reached in investigations of the gravitational sedimentation which is characterized by the constant gravitational forces. The question of the centrifugal sedimentation when the external forces acting on suspension essentially exceed the gravity and change in the time is not deeply investigated theoretically and experimentally. In the present paper, we construct a mathematical model of the centrifugal sedimentation of dilute suspensions, apply this model to diamond and Ti_3SiC_2 particles and compare the theoretical results to the experiments.

Taking into account hydrodynamic interactions of particles and the effect of walls it is possible to correct formula (1). One can find various modifications in [6] and papers cited therein. In the present paper, we use the Barnea-Mizrahi correction

$$U = U_s \frac{(1-\phi)^2}{(1+\phi^{1/3}) \exp\left[\frac{5\phi}{3(1-\phi)}\right]} \tag{2}$$

Where ϕ denotes concentration

We have chosen formula (2), since it gives more realistic results than other corrections [6] in our experiments presented below. It is worth noting that sedimentation for higher concentrations ϕ are described by non-linear parabolic equations . Dilutent suspensions when ϕ is small are sufficiently well described by equation (2). In the present paper, we consider the case ϕ = 0.1, hence formula (2) can be assumed as the benchmark of our further calculations.

The high-speed centrifugal settling requires verification of the theoretical results based on formulas (1)-(2), since the gravitational acceleration g_0 is replaced by the centrifugal acceleration g which exceeds g_0 at least five times. Moreover, the centrifugal acceleration depends on time t. We discuss these theoretical questions in Sec. 2 and 3. In Sec. 4 new formulas for the high-speed centrifugal settling are deduced and applied to High Speed Centrifugal Compaction Process.

2. Description of the mathematical model

2.1. Geometry of vessel

The geometrical scheme of the volume is presented in Fig. 1. It is a tube vessel with the circular base. The distance between the centre of rotation and the top of the vessel is denoted by $r_{\min}$ and fixed equal to 5.5 *cm*. The distance to the bottom $r_{\max}$ is equal to 12.88 *cm*. So, the height of the vessel is 7.38 *cm*. The axis of rotation is perpendicular to the axis of the tube.

Spherical particles are uniformly distributed in the vessel, hence we have at the initial time $t = 0$ a uniform suspension. At the beginning of the experiment the gravitational forces act to the particles but not essentially change their position. In the process of the accelerated rotation the centrifugal forces exceed the gravitational forces more than five times. This implies that the particles fall from the top to the bottom of the vessel and the gravitational effects can be neglected in such experiments.

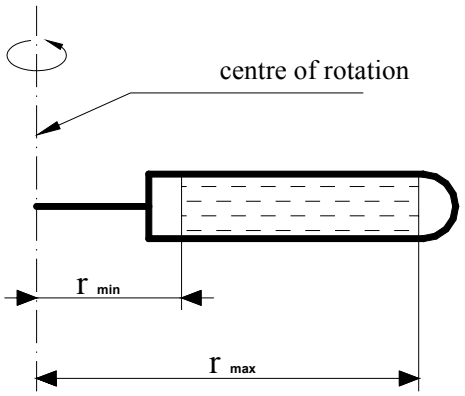

Fig. 1. The geometrical scheme of the rotor

2.2. Non-stationary sedimentation

In order to apply formulas (1)-(2) to the high-speed centrifugal sedimentation we have to make modifications. First, the constant g_0 is replaced by the function $g(t) = r(t)\omega^2(t)$, where $r(t)$ is the distance which a particle passed from the top $r_{\min} = 5.5\,cm$ of the vessel to the bottom at the time t; $\omega(t)$ is the angular velocity. A typical plot of $\omega(t)$ is given in Fig. 2.

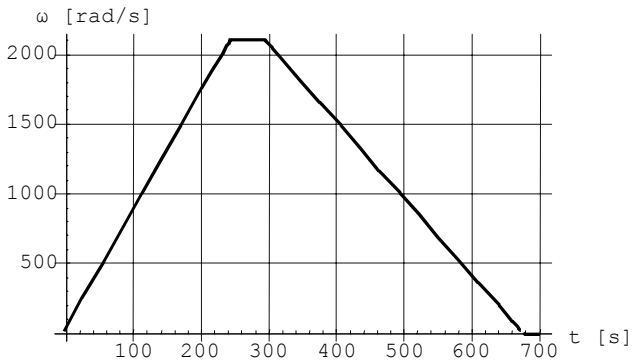

Fig. 2. Dependence of the angular velocity ω on the time t. Time of acceleration t_1 = 247 s, time of constant angular velocity t_2 = 50 s, time of braking t_3 = 380 s, constant angular velocity 20000 rpm

The function $\omega(t)$ is piecewise linear and has the form

$$\omega(t) = \begin{cases} a_1 t, & 0 \le t < t_1, \\ \omega_0, & t_1 \le t < t_2, \\ a_2 t + b, & t_2 \le t < t_0, \end{cases} \tag{3}$$

where t_1 is the time of acceleration, $t_2 - t_1$ the time of constant angular velocity, $t_0 - t_2$ the time of braking, t_0 the total time of the process; a_1, a_2 and b are appropriate constants.

Equations (1)-(2) become

$$U(t) = \frac{d^2(\rho - \rho_c)}{18\eta} \frac{(1-\phi)^2}{(1+\phi^{1/3})\exp\left[\frac{5\phi}{3(1-\phi)}\right]} r(t)\omega(t), \tag{4}$$

where $U(t)$ denote the velocity of the particle at the time t. Using the relation $\frac{dr}{dt}(t) = U(t)$ we arrive at the linear differential equation of first order

$$\frac{dr}{dt}(t) = \frac{d^2(\rho - \rho_c)}{18\eta} \frac{(1-\phi)^2}{(1+\phi^{1/3})\exp\left[\frac{5\phi}{3(1-\phi)}\right]} r(t)\omega(t), \tag{5}$$

with the initial condition $r(0) = r_{\min}$. Applying the method of separated variables we obtain

$$r(t) = r_{\min} \exp\left[\frac{d^2(\rho - \rho_c)}{18\eta} \frac{(1-\phi)^2}{(1+\phi^{1/3})\exp\left[\frac{5\phi}{3(1-\phi)}\right]} \Omega(t)\right], \tag{6}$$

where

$$\Omega(t) = \int_0^t \omega^2(\xi)\,d\xi .$$

The latter integral is easily calculated for the function $\omega(t)$ given by (3)

$$\Omega(t) = \begin{cases} \frac{a_1^2}{3} t^3, & 0 \le t < t_1, \\ \frac{a_1^2}{3} {t_1}^3 + \omega_0^2 t, & t_1 \le t < t_2, \\ \frac{a_1^2}{3} {t_1}^3 + \omega_0^2 t_2 + \frac{a_2^2}{3} t^3 + a_2 b t^2 + bt, & t_2 \le t < t_0 \end{cases} \tag{7}$$

Using formulas (3)-(7) we can determine the path $r(t)$ of any particle (see example in Fig. 4).

Formula (6) is valid up to $t = t_0$ when the function $r(t)$ attaches the maximal value $r(t_0) = r_{\max} = 12.88$ (8) corresponding to the bottom of the vessel. The relation (8) can be considered as a number equation with respect to t_0. This equation is easily solved by the method of successive approximations, since the derivative $\frac{dr}{dt}(t) = U(t)$ is a positive function (see (4)), hence $r(t)$ is an increasing function. Thus, equations (6)-(8) produce an algorithm to compute the settling time t_0 of the particle of the diameter d. Considering t_0 as a function

$t_0 = t_0(d)$ we can estimate the sedimentation regime of the particles of different sizes. Example is presented in Fig. 3.

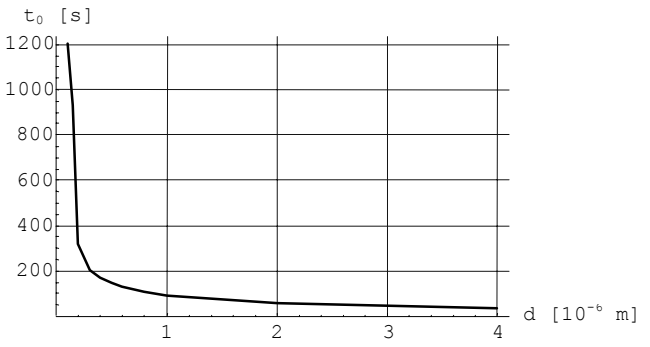

Fig. 3. Dependence of the settling time t_0 on d for Ti_3SiC_2

One see at Fig. 3 instability of the dependence $t_0 = t_0(d)$ near the point $d = 0.3 \cdot 10^6 m$, i.e., small perturbations of the diameter d produce large deviations of t_0. This fact can be essential for small particles, because the distribution of the sizes is tabulated with an error which can drastically change the time of settling. Here, the diffusion processes which can take place for small particles submicrometric or nanometric [17] are not taken into account.

Consider many spherical particles of different sizes made from the same material. Using equations (6)-(8) one can observe the details of the polydisperse settling and its dependence on the size of the particles. An example of the Ti_3SiC_2 particles is presented in Fig. 4. One can see that not all particles of the diameter $d = 0.15$ reach the bottom during the process.

The ratio $\dfrac{r_{\max} - r(t_0)}{r_{\max} - r_{\min}}$ corresponds to the part of not settled particles to the end time t_0. The ratio settled and non-settled particles is equal to the ratio of the vertical segments cut by the curve $r(t)$ for $d = 0.15$ at the time t_0.

It is convenient to use the discrete density distribution of the sizes $(d_i, \Delta n_i)$, $i = 1,2,...,n$, where d_i denotes the diameter of the i-th particle, Δn_i the ratio of the number of particles with the diameter d_i to the total number of particles.

Introduce a value M_0 proportional to the total mass of particles

$$M_0 = \sum_{i=1}^{n} d_i^3 . \tag{9}$$

The part of the mass of the settled particles $W(t)$ at the time t is calculated by formula

$$W(t) = \frac{1}{M_0} \sum_{r_i = r_{\max}} d_i^3 , \tag{10}$$

where the sum in (10) is taken over all $r_i(t)$ equal to $r_{\max}$. Here $r_i(t)$ is calculated by (6)-(7) with $d = d_i$. An example of the function $W(t)$ is presented in Fig.5. Here, the computations are performed for the diamond particles. The distribution of the particles $(d_i, \Delta n_i)$ were measured by Shimadzu's apparatus. It is presented at Fig. 6.

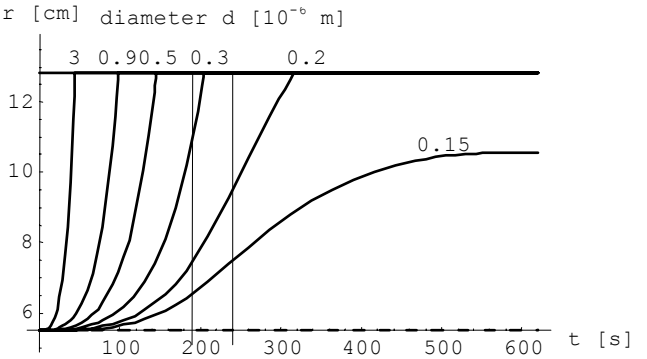

Fig. 4. Path *r(t)* calculated by (6)-(8) for various *d*. Regime of rotation is described in Fig.1. Two vertical lines near *t* = 200 corresponds to the change of the angular velocity

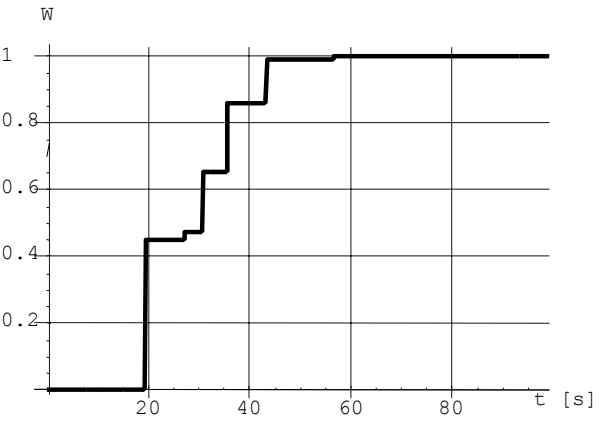

Fig.5. Dependence of the concentration *W* on *t* for diamond powder for the regime of rotation described in Fig.1

The proposed method can be developed to particles made from different materials. Let us take two different materials: diamond ($\rho = 3.515\ g/cm^3$) and Ti_3SiC_2 ($\rho = 4.53\ g/cm^3$). Let the total masses of diamond and of Ti_3SiC_2 are equal. Introduce the parts of the total mass of all settled particles $W_d(t)$ and $W_T(t)$ for diamond and Ti_3SiC_2, respectively, by formula (10) with the coefficients 0.5. Then

$$W(t) = \frac{W_d(t)}{W_d(t) + W_T(t)} , \tag{11}$$

is the part of the diamond particles settled at the time *t*. One can see that (11) corresponds to the mass intensity of the settled diamond particles at the time *t*, hence, it equals to the concentration of the graded compaction produced by centrifugal sedimentation. An example of $W(t)$ for diamond-Ti_3SiC_2 compacts is presented in Fig. 7.

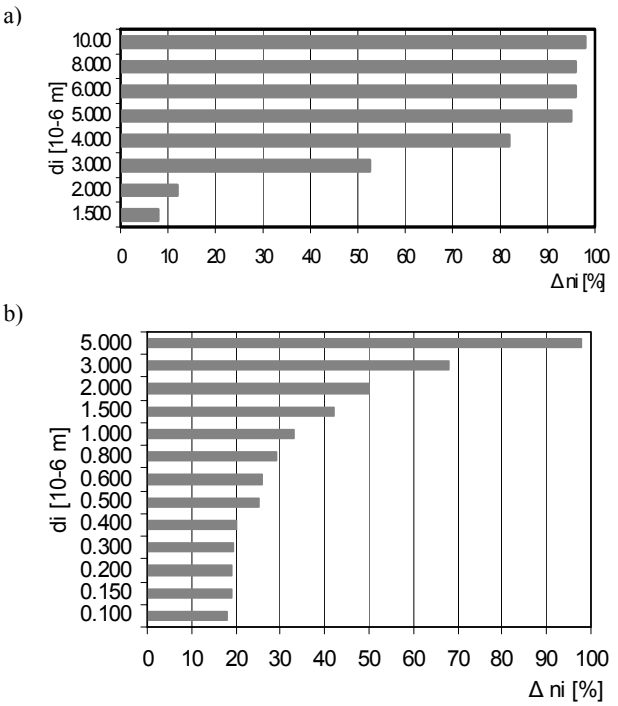

Fig. 6. Distribution of the particles $(d_i, \Delta n_i)$ measured by Shimadzu's apparatus for diamond (a) and Ti_3SiC_2 (b)

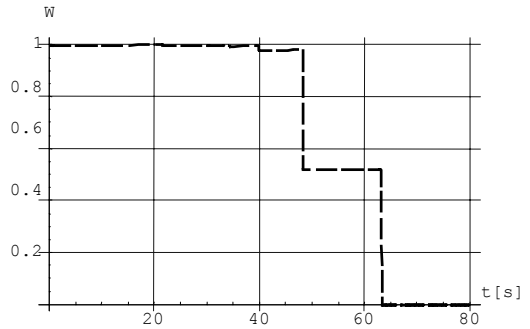

Fig. 7. Function *W(t)* from (11) for diamond-Ti_3SiC_2 compacts diamond for the regime of rotation described in Fig.1

Let T_0 be the time when the first particles reach the bottom of the vessel. Then the concentration of settled diamond at the time *t* is described by the function

$$c_d(t) = W\left(\frac{l}{L}(t_0 - T_0) + T_0\right), \tag{12}$$

where *L* denotes the ultimate height of the graded material in the vessel.

3. Analysis of Reynolds and Froude numbers

The effect of finite size of the vessel implies that the liquid is going to the opposite side to the falling particles with the average velocity $U_l(t) = \frac{\phi}{1-\phi}U(t)$, where $U(t)$ is the velocity of particles, ϕ is the concentration of the particles in fluid. Locally the velocity of the fluid can exceed $U_l(t)$, for instance for close particles generating a cloud [13]. Polydispersity also can increase the local velocity [10]. Consider the Navier-Stokes equations which describe quasi stationary flows in viscous fluidł.

$$\mu\nabla^2 u = \nabla p + \rho(u\cdot\nabla u) - \rho g\,, \nabla u = 0, \tag{13}$$

where *u* denote the local velocity, μ the cinematic viscosity. Dimensionless form of equations (13) can be written as follows [14]

$$\nabla^2 u' = \nabla p' + \mathrm{Re}(u'\cdot\nabla u') - \frac{\mathrm{Re}}{Fr^2}e, \,, \nabla u' = 0, \tag{14}$$

where $Fr = \frac{U_l}{\sqrt{gL}}$ is the number of Froude, the unit vector *e* is directed to bottom of the vessel. Frequently, the gravitational forces in equations (14) are omitted, since the gravitational acceleration *g* is small. This implies that the Froude number is large and the last term in the first equation of (14) is less than others. However, for high-speed centrifugal rotations the centrifugal acceleration is large. Then the Froude number becomes small and even for moderate **Re** the third term in the first equation of (14) can exceed other terms. This yields another type of instability not related to the inertial terms (Reynolds number). Usually the gravitational forces serve as a factor increasing stability. In the linear case of (14) when **Re** can be taken as zero, a solution of the partial differential equations is proportional to the ratio $\frac{\mathrm{Re}}{Fr^2}$.

For the regime presented in Fig. 1 **Re** is of order 0.001 and $\frac{\mathrm{Re}}{Fr^2}$ is of order 10^7. Therefore, the viscous flow is laminar, but the large value of $\frac{\mathrm{Re}}{Fr^2}$ yields high deviation of the local velocity *u* which can occur despite of the theoretical stability of equations. However, due to the high-speed centrifugal rotation which yields the stratification of the liquid layers by the depth, we have stable situation for the Navier-Stokes equations (14).

4. Experimental investigation of the graded materials

Method of powders consolidation has a significant influence to microstructure and materials properties. The best compaction is achieved for centrifugal compaction of suspensions which consist of fine powders (High Speed Centrifugal Compaction Process, HCP). We used the centrifuge UP 65M with rotational speed from

15000 to 25000 rpm, for different total times of the sedimentation process. Macrostructure of the FGM diamond–Ti_3SiC_2 composite is presented in the Fig. 8. It was obtained during 50 s with constant angular velocity 20000 rpm.

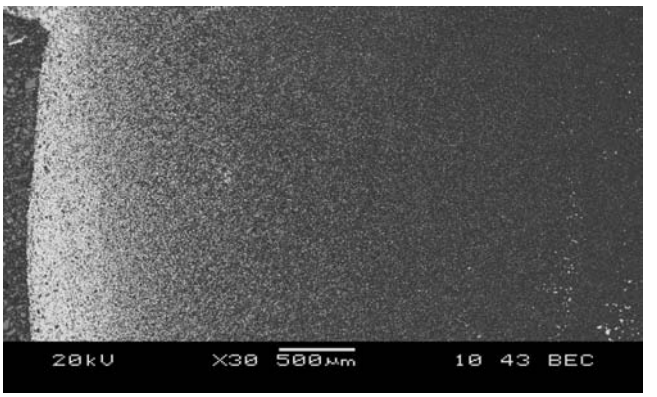

Fig. 8. Macrostructure of the FGM diamond-Ti_3SiC_2 composite

The measured hardness gradient is presented in Fig. 9 from the top surface to the bottom surface of the sample.

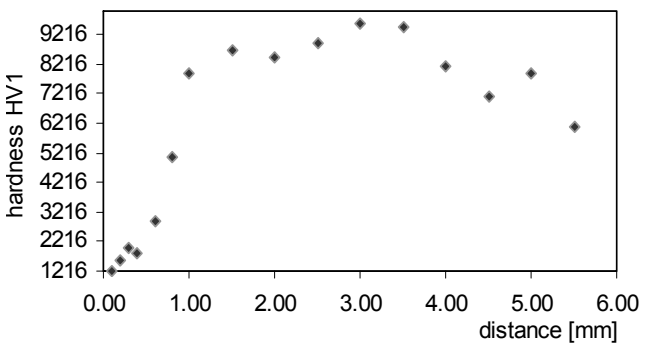

Fig. 9. The hardness distribution in the diamond composite with graded microstructure

5. Conclusions

In this paper, we construct a mathematical model of FGM basing on the modifications of the Stokes formula. We proposed an algorithm to describe sedimentation of the group of spherical particles of different sizes and different materials. The results are applied to diamond-Ti_3SiC_2 suspensions to produce graded compacts.

The results presented in Fig. 5 demonstrate that for the considered diamond-Ti_3SiC_2 suspensions the obtained compact has the structure of the laminate, i.e., the layer of pure diamond transforms into the layer of pure Ti_3SiC_2 with the small layer containing 50% of the both materials. Simulations show that it is possible to obtain continuous concentrations of the both materials with appropriate initial suspensions. Thus, this method allows to obtain graded materials with slowly changing of the local properties.

Acknowledgements

This work were supported by the Ministry of Science and Higher Education of Poland under the project No. N508 011 31/0931.

References

[1] R. Borchert, N. Willert-Porada, An oxidation resistant metal - ceramic functionally graded material, Proceedings of the Conference "90th Cimtec-World Ceramics Congress, Getting into the 2000's – Part C", TECHNA, 1990, 313-320.
[2] L. Jaworska, M. Rozmus, B. Królicka, A. Twardowska, Functionally graded cermets, Journal of Achievement in Materials and Manufacturing Engineering 17 (2006) 73-76.
[3] G. Matula, L.A. Dobrzański, Structure and properties of FGM manufactured on the basis of HS6-5-2, Journal of Achievements in Materials and Manufacturing Engineering 17 (2006) 101-104.
[4] M. Mirzababaee, M. Tahani, S.M. Zebarjad, A new approach for the analysis of functionally graded beams, Journal of Achievement in Materials and Manufacturing Engineering 17 (2006) 265-268.
[5] L.A. Dobrzański, A. Kloc, G. Matula, J. Domagała, J.M. Torralba, Effect of carbon concentration on structure and properties of the gradient tool materials, Journal of Achievement in Materials and Manufacturing Engineering 17 (2006) 45-48.
[6] J. Bandrowski, H. Merta, J. Zioło, Sedimentation of suspention, Silesian University of Technology Press, Gliwice, 2001.
[7] R.B. Jones, R. Kutteh, Sedimentation of colloidal particles near a wall, Stokesian dynamic simulations, Journal of Physical Chemistry 1 (1999) 2121-2139.
[8] M.L. Ekel-Jeżewska, B. Metzger, E. Guazzelli, Spherical cloud of point particles falling in a viscous fluid, Physical Fluids 18 (2006) 123-130.
[9] T. Bosse, L. Kleiser, E. Meiburg, Small particles in homogeneous turbulence: Settling velocity enhancement by two-way coupling, Physical Fluids 18 (2006) 1-18.
[10] M.P. Brenner, Screening Mechanisms in Sedimentation, Phys. Fluids 11 (1999) 754-772.
[11] A.J.C. Ladd, Effects of container walls on the velocity fluctuations of sedimenting spheres, Physical Review Letters 88 (2002) 1-4.
[12] H. Nicolai, Y. Peysson, É. Guazzelli: Velocity fluctuations of a heavy sphere falling through a sedimenting suspension, Physical Fluids 8 (1996) 855-862.
[13] E.Guazzelli, Evolution of particle-velocity correlation in sedimentation, Physical Fluids 13 (2001) 1537-1540.
[14] P.J. Mucha, S.Y. Tee, D.A. Weitz, B.I. Shraiman, M.P. Brenner, A model for velocity fluctuations in sedimentation, Journal of Fluid Mechanic 501 (2004) 71-104.
[15] N.Q. Nguyen, A.J.C. Ladd, Sedimentation of hard-sphere suspensions at low Reynolds number, Journal of Fluid Mechanic 525 (2005) 73 -104.
[16] M.C. Bustos, R. Burger, F. Concha, E.M. Tory, Sedimentation and Thickening, Kluwer Academic Publ. Dordrecht, 1999.
[17] S. Ramaswamy, Issues in the statistical mechanics of steady sedimentation, Advances in Physics 50 (2001) 341-345.